Epitaxial growth of Ag on W(110)

C. Deisl and E. Bertel
Institut für Physikalische Chemie, Universität Innsbruck, A-6020 Innsbruck, Austria

M. Bürgener, G. Meister, and A. Goldmann
Institut für Physik, Universität Kassel, D-34132 Kassel, Germany
(Received 2 February 2005; revised manuscript received 30 June 2005; published 26 October 2005)

Epitaxial growth of Ag on W(110) at room temperature was studied by scanning tunneling microscopy (STM) and polarization-dependent photoemission. At coverages far below one monolayer Ag atoms populate bcc sites of the substrate and form close-packed islands of monolayer thickness. With increasing coverage geometrical misfit between Ag(111)-like layers and W(110) generates surface stress along W[$1\bar{1}0$]. This is released by formation of domain walls parallel W[001] which are observed with a distance between about 25 Å and 30 Å, depending on the details of the growth process. At one monolayer coverage most of the Ag atoms still reside in or very near to bcc substrate positions, but now the strain release pattern is changed: solitons aligned along W[$\bar{1}12$] are formed at an average distance between 35 Å and 50 Å. The details of the soliton arrangement depend critically on the degree of equilibration and the presence of holes in the monolayer film which allow an additional stress release. This is evident from a comparison with results of STM studies performed at the closed and carefully annealed Ag monolayer [Kim *et al.*, Phys. Rev. B **67**, 223401 (2003)]. Further deposition of Ag starts growth of a second monolayer by formation of islands which increase in size with coverage. At a nominal coverage of 1.5 monolayers the strain relieve pattern changes again: some corrugation lines are oriented along W[001] as in the submonolayers, but other orientations related to Ag(111) directions appear as well. This indicates that several possibilities are available at similar energy costs and that the transition from the W substrate potential to a Ag potential seen by the second layer is very soft. Finally at a nominal coverage of several monolayers, Stranski-Krastanov growth is observed producing Ag(111)-like terraces with one of the dense-packed Ag rows oriented parallel to W[$1\bar{1}1$].

DOI: 10.1103/PhysRevB.72.155433 PACS number(s): 68.37.−d

I. INTRODUCTION

Low-dimensional metal-on-metal systems are presently a topic of great interest in the context of "materials tailoring." In contrast to solids in the bulk, where not much room exists to manipulate the self-consistent balance between geometrical and electronic structure, ultrathin overlayers [generally called two-dimensional (2D) for simplicity], chain structures (1D), and more complex low-dimensional arrangements grown on single-crystal surfaces of a different substrate material offer a wide playground to vary the subtle balance between various relevant interactions.[1–4] One of the decisive parameters is the match (or mismatch) of the substrate surface lattice and the lattice with which the material deposited in heteroepitaxy likes to grow in its bulk. Next there are forces acting normal to the surface between adsorbate and substrate as well as forces operating laterally within the growing overlayer. In other words, the final growth mode of the first adsorbed monolayer (ML) will be determined by the mechanical surface stress distribution within the heteroepitaxial system. In consequence there may be a variety of growth possibilities such as coincidence structures, pseudomorphic structures, and the formation of complex misfit dislocation networks. Small changes in external parameters may switch the system from one mode into the other. This provides a possibility of tuning into different structures, of creating templates with larger periodicities for self-organized cluster growth, or making use of enhanced reactivity in strained overlayers.[5] On the other hand, the sensitivity to variations of external parameters poses a serious challenge for the controlled growth and the stability of nanostructures. Moreover, the growth mode may change drastically from layer to layer if, as to be expected generally, the stress-distribution field varies with the amount of deposited material. To summarize, the motivation to study growth of ultrathin metal overlayers on metallic substrates is manifold. Besides the challenge to understand quantitatively the transition from submonolayer adsorption to the multilayer film representing bulk properties (3D), the interaction of ultrathin overlayers with gaseous adsorbates may be very different both from the clean surface of the substrate as well as clean single-crystal surfaces of the adsorbate material. The latter effects give hope that also reaction steps, e.g., in heterocatalytical processes may be tailored by adequate combinations of materials.[6] Finally, the study of growth, kinetics, and dynamics of ultrathin layers is crucial for the understanding and control of the growth and the stability of nanostructures.

The particular example of Ag on W(110) has attracted continuous interest over the years.[7–11] The metallic radius of Ag (fcc, lattice constant $a=4.09$ Å) exceeds that of W ($a=3.16$ Å, bcc). Therefore Ag is not expected to grow pseudomorphically. Indeed the complex low-energy electron diffraction (LEED) patterns observed in their dependence on Ag coverage were interpreted[7] by incommensurate layer formation. For example, the first monolayer was considered as an approximate (111) plane, that is dilated in the [001] direc-

tion of the substrate to fit its periodicity and compressed in the $[1\bar{1}0]$ direction to partially compensate for the reduced packing density.[7] Both LEED and Auger spectroscopy studies demonstrate the growth of a second layer on top of the essentially closed first one.[7,9] Thermal desorption spectra[7] show that the first two layers are stable up to their desorption temperature T_d, but with the second layer (T_d=1070 K) bound less strongly than the first one (T_d=1160 K). The buckling of the first layer was studied with helium atom diffraction.[11] It was found to be 0.08 Å, i.e., smaller than expected from a hard-sphere model. The structural analysis[11] indicates an expansion along [001] (contraction along $[1\bar{1}0]$) of the real-space surface unit cell of 10% (3%) at most.[11] Although the geometry parameters derived[11] differ only slightly from the LEED analysis,[7] the general agreement is less satisfying. Angle-resolved photoemission spectroscopy[12–14] gives additional strong evidence for the layer-by-layer growth modes up to 2 ML as derived in Refs. 7–11. Moreover it reveals clearly that monolayer Ag films are converted into double-layer Ag islands by exposition to 20 L (1 L=10^{-6} Torr s) of molecular oxygen at room temperature.[12,14] This oxygen-driven geometrical rearrangement is of interest in the context of thin-film-adsorbate interaction and stimulates us to explore the growth modes of Ag on W(110), both with and without interaction with oxygen, in more detail using scanning tunneling microscopy (STM). In fact, all methods discussed above are laterally integrating over a millimeter scale. It is therefore difficult or impossible to extract the very details such as shape of growing ML islands, remaining holes within the film, and any nonperiodic structures occurring on the nm scale. The closed first epitaxial layer of Ag on the W(110) surface was also studied with STM by Kim *et al.*[15] in detail. As in their previous work the films were annealed and the structures reported by these authors are close to the equilibrium structure of the perfect Ag monolayer. The present paper reports our results on the growth of Ag on W(110) at or slightly above room temperature. As it turns out, there are a variety of metastable and defect-rich structures. In this sense the present work closes the gap between the early LEED (Ref. 7) and He scattering[11] studies of the Ag submonolayer and monolayer growth, which at least in part concerned also kinetically determined structures and the recent STM study[15] by Kim *et al.*, which addressed the full monolayer at or close to equilibrium.

II. EXPERIMENT

All STM experiments were carried out in Innsbruck in an UHV chamber with a base pressure $p<8\times10^{-11}$ mbar. It was equipped with an STM (Rasterscope 3000 of DME, operated with an RHK SPM 100 electronics and an electrochemically etched tungsten tip), LEED (ErLEED 3000 D, Vacuum Science Instruments Ltd.), a mass spectrometer, and an indirectly heated alumina crucible for evaporation of Ag. The W(110) sample was a circular disk of 8 mm diameter, oriented to better than 0.25°, which corresponds to an (experimentally verified) terrace width of several hundred angstroms. Cleaning was accomplished by repeated heating to T=1400–1750 K in 5×10^{-8} mbar of O_2, followed by a rapid flash to T=2300 K in the absence of oxygen. Insufficient cleaning resulted in very small, but ordered carbon islands on the terraces, which were too small to be detected by Auger electron spectroscopy, but were immediately detectable in STM after deposition of silver, because it led to a characteristic agglomeration of the Ag atoms into small clusters. If the temperature reached in the final flash was not high enough, one could also detect small islands of partially oxidized W in STM. This too, resulted in Ag clustering. After successful cleaning no indications for the well-known[16] C-induced reconstructions on W(110) could be detected in the atomically resolved STM image and a brillant substrate LEED pattern with very low background intensity was observed. All images were obtained at RT. The constant current mode was used with 0.04–0.6 eV positive or negative tip bias and tunnel currents of 0.1–0.7 nA. Ag was evaporated at a constant rate of 0.7 ML per minute, with the substrate at or slightly above RT.

The photoemission experiments were carried out in Kassel in an apparatus described in detail elsewhere.[17] It is equipped with LEED and a high-resolution photoelectron spectrometer combined with a source of linearly polarized (92%) Helium resonance radiation ($\hbar\omega$=21.2 eV). Details concerning sample preparation, coverage calibration and, in particular, the interpretation of normal-emission photoelectron spectra from the Ag/W(110) system in terms of growth mode are published in considerable detail in Refs. 12–14.

III. RESULTS AND DISCUSSION

A. Overview

An overview of growth behavior up to 1 ML is given in Fig. 1. Quite surprising we find two different growth modes, depending on very subtle and not clearly identified differences in substrate preparation. The growth process either starts at steps [Fig. 1(a)] where rather large islands of 1 ML thickness nucleate. Alternatively, nucleation starts off the steps on terraces [Fig. 1(c)] by forming islands with a fractal-like structure. In the latter case nucleation at steps is avoided, indicating a limited area which supplies Ag atoms for the further growth of the islands. The Ag atoms do not leave the terrace on which they landed. The shape of the "fractal islands" is somewhat in between the dendrites observed for the growth of Au on Ru(0001) by Behm and co-workers[25] and the more "wormlike structures" reported by Thürmer *et al.* for Ag on Si(111).[26] Their slightly rounded shape indicates that edge diffusion is not negligible at room temperature and modifies the dendritic shape expected for purely diffusion limited aggregation.[25] Furthermore, a detailed analysis of the shape of the "fractals" indicates that they are composed of smaller, almost rectangular, subunits. This is a clear hint of a strained structure, which is divided into small domains by a trench network. We come back to this later in the paper.

We observe strong chemical contrast between W and Ag; compare Fig. 1. The apparent corrugation measured along the white line in Fig. 1(a) is reproduced in Fig. 1(b). The height of a step on W(110) is 2.24 Å and was used to calibrate the vertical scale of the STM. Obviously the apparent

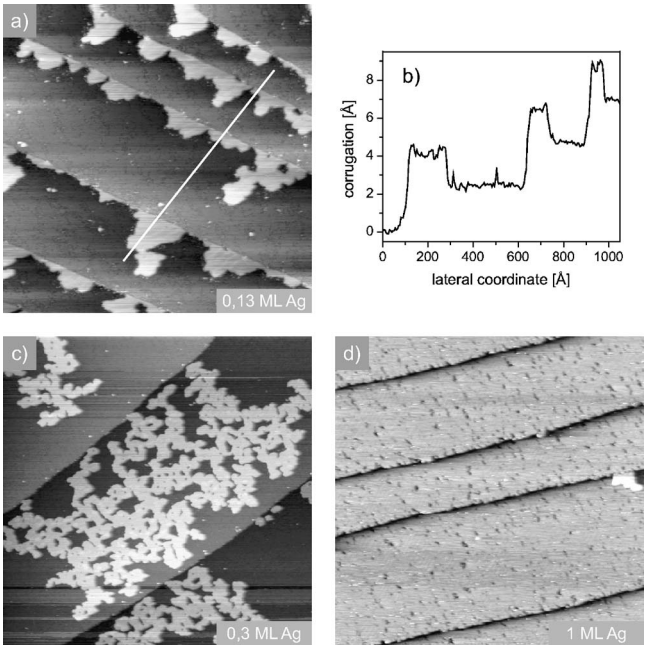

FIG. 1. Epitaxial growth of Ag on W(110) starts either at steps (a) or on terraces (c) at submonolayer coverage. Apparent corrugation along the white line in (a) is reproduced in (b). The STM image of the almost closed first monolayer is shown in (d). Data for tip bias, tunnel current, and length scales are (a) −180 mV, 0.54 nA, 1400×1400 Å^2, (c) 289 mV, 0.31 nA, 2800×2800 Å^2, and (d) 39 mV, 0.28 nA, 3500×3500 Å^2.

corrugation above Ag strongly exceeds the atomic diameter $d=2.88$ Å of Ag in the fcc bulk lattice. This is clearly not a geometric but rather an electronic effect. In principle, it could be due to a much larger local density of states above the Ag island. However, this explanation seems unlikely, because a similar height difference also appears in Fig. 1(c), which was recorded with a totally different bias voltage. More likely, the apparent corrugation difference results from the difference in the work function of W and Ag. For W(110) the work function is 5.1 eV, whereas Ag(111) has a work function of 4.72 eV (Ref. 27). Of course, the work function of an Ag monolayer island is not necessarily the same as of bulk Ag(111), but a significant work-function difference between W and Ag can be inferred from these data in any case. The smaller work function of Ag translates into a smaller barrier height in the tunneling experiment.

As mentioned, initial growth of one layer thick islands may proceed alternatively via the two mechanisms shown in Figs. 1(a) and 1(c). One might argue that contamination with atomic H leads to a blocking of step sites for nucleation. We have, however, no experimental evidence for this. Rather we believe that the differences are due to slightly different substrate temperatures during deposition. At slightly higher temperatures stable nuclei are only formed at step sites, while at lower temperatures stable nuclei can form on the terraces. In the latter case the island growth slows down and eventually stops in front of steps because the capture zone is limited by the step and tends to zero as the island approaches the step edge. In both cases shown in Figs. 1(a) and 1(c) further deposition of Ag atoms subsequently fills the uncovered regions of the substrate until finally an almost closed first ML of Ag is formed, see Fig. 1(d). The resulting concentration of defects (holes) is about 2.5% of the ML area. Further deposition of Ag does not fill the holes but starts growth of the second layer. After the second layer is almost filled (it retains the holes of the first ML) we observe 3D (Stranski-Krastanov) growth, in agreement with the earlier experiments. A typical STM result is reproduced in Fig. 2(a), corresponding to an average coverage of 4 ML. The measured corrugation as displayed in Fig. 2(b) indicates a hole about 16 Å deep which corresponds to six layers. Up to now all our results are consistent with the earlier experiments using diffraction techniques[7–9,11] and angle-resolved photoemission.[12–14]

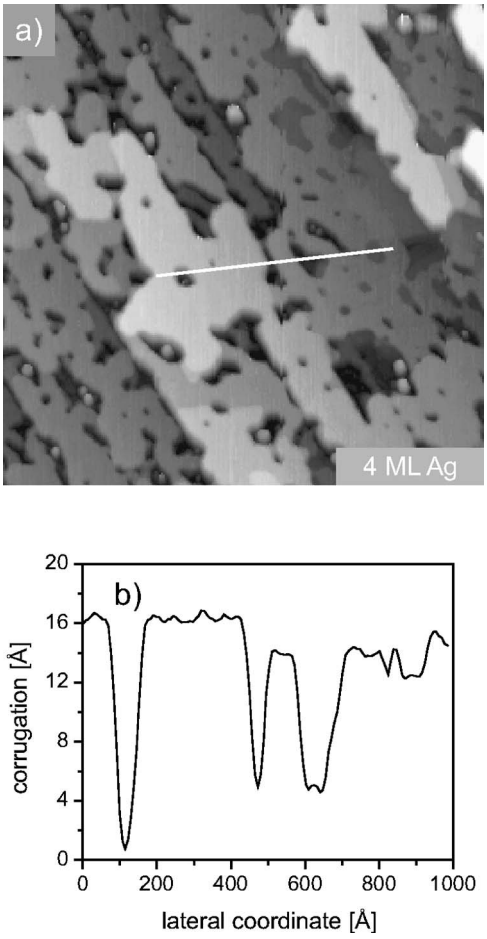

FIG. 2. Stranski-Krastanov growth of nominally 4 Ag monolayers on W(110) is shown in (a). The experimental corrugation along the white line in (a) is reproduced in (b). Experimental tip parameters and scale are 178 mV, 0.26 nA, and 1950×1950 Å^2.

Despite the significant corrugation and simultaneous growth of different layers as revealed in Fig. 2 large terraces oriented parallel to the substrate terraces are produced. This is shown more clearly in Fig. 3(a). On these terraces atomic resolution is easily obtained (in contrast to the first ML) and Fig. 3(b) indicates already the formation of Ag(111)-like planes. Further growth at increasing nominal coverage leads to approach the geometrical and electronic structure of the Ag(111) surface. This has indeed been observed in normal-

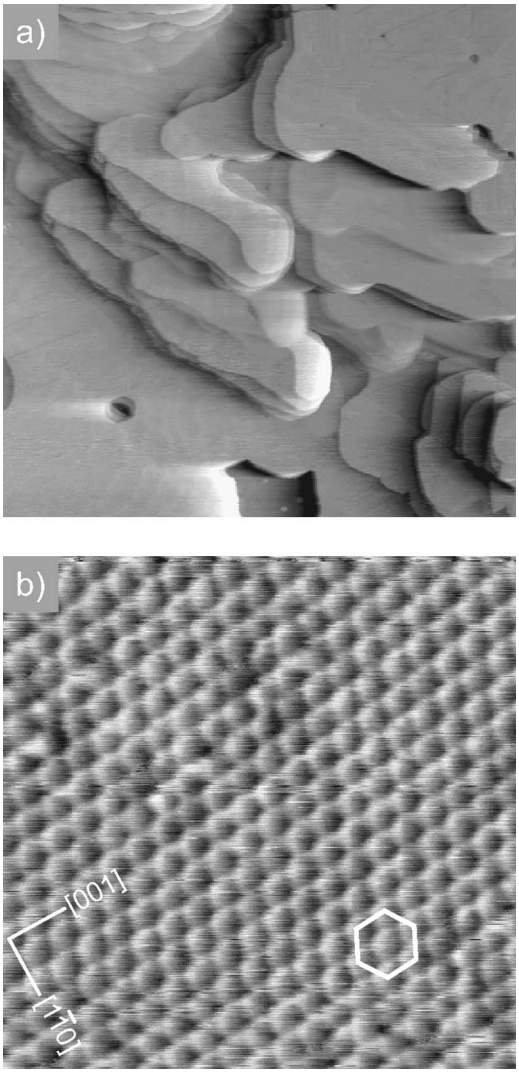

FIG. 3. Growth of nominally 6 Ag monolayers on W(110) is shown (high-pass filtered) in (a). A zoom into (a) with atomic resolution is reproduced in (b). It indicates an almost ideal Ag(111) layer in the Kurdjumov-Sachs orientation with one of the dense-packed Ag rows oriented parallel to W[1$\bar{1}$1]. Coordinates in (b) give the substrate orientation. Experimental parameters are (a) 289 mV, 0.43 nA, and 4200×4200 Å^2, (b) −138 mV, 0.66 nA, and 55×55 Å^2.

emission photoelectron spectra, which reproduce very clearly[12,13] all details well known from Ag(111) and also clearly show the Shockley-type surface state at $\bar{\Gamma}$ about 60 meV below E_F.[18]

B. Atomic structure

Closer inspection of submonolayer islands shows a characteristic stripe pattern, producing valleys along the [001] substrate direction and a corrugation about 0.2 Å deep along [1$\bar{1}$0]. A typical result is displayed in Fig. 4, where the corrugation [Fig. 4(b)] is shown along the black line drawn in Fig. 4(a). The corrugation is nearly periodic with an average distance of the troughs of about 29 Å. This result is fully

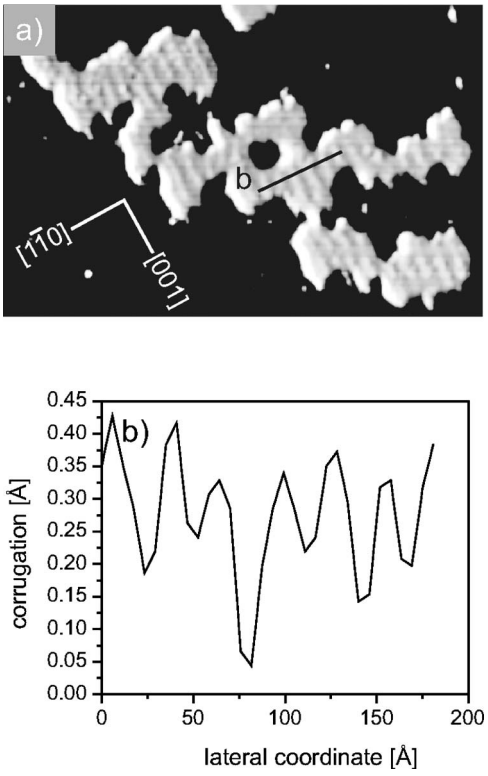

FIG. 4. Submonolayer islands of Ag on W(110) show a characteristic stripe pattern along the [001] substrate direction (a). The measured corrugation along the black line in (a) is reproduced in (b). Experimental data for tip bias, tunnel current, and length scale are 198 mV, 0.38 nA, and 640×920 Å^2.

consistent with the experimental LEED data:[7] these reveal superstructure spots along [$\bar{1}$10] and their position indicates a superimposed periodicity of about 27 Å. Bauer *et al.*[7] interpret their data by the presence of an incommensurate Ag layer with a rigid lattice and a laterally deformed Ag(111) unit cell. It is rotated with respect to the substrate according to the Nishiyama-Wassermann orientation,[19] i.e. Ag[1$\bar{1}$0]$\|$W[001], slightly dilated ($\approx$9%) along W[001] and somewhat compressed ($\approx$4%) along W[$\bar{1}$10]. This incommensurate lattice then produces the corrugation with a repetition every 27 Å. We argue for a different interpretation in the following.

A theoretical study based on a nonadditive effective binding potential calculates the lateral dependence of the Ag binding energy on the W(110) adsorption site.[10] At the bridge site (along [1$\bar{1}$1] and equivalents) the energy surface forms a saddle point with a relatively narrow minimum of 3.04 eV along [1$\bar{1}$1]. As expected the on-top position is energetically unfavorable with 2.56 eV. In contrast, the bcc site (hollow site along [1$\bar{1}$0] and [001]) is preferred by a binding energy of 3.28 eV. The energy surface around the bcc site is quite flat along [1$\bar{1}$0] and allows an individual adsorbed Ag atom to move almost freely along a path of about ±0.5 Å. Even a shift of ±0.7 Å changes the binding energy by $\lesssim$0.08 eV. A consideration of total energy, therefore, clearly favors that most Ag atoms adsorb in bcc sites as compared to an incom-

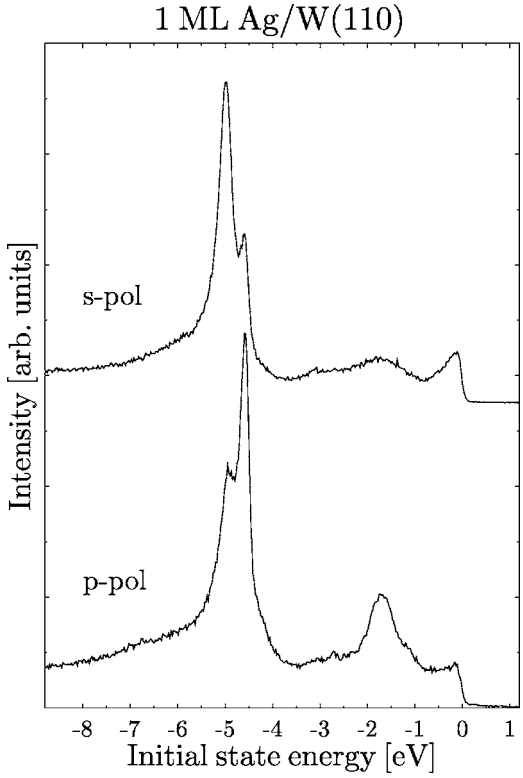

FIG. 5. Normal emission valence band photoelectron spectra taken with 95% linearly polarized light at $\hbar\omega$=21.2 eV. Photon incidence at 45° along the $[1\bar{1}0]$ azimuth of a W(110) sample covered with one monolayer of Ag. Top *s*-polarized, bottom *p*-polarized radiation.

mensurate rigid Ag layer which necessarily includes many near bridge and near on-top sites. Qualitatively identical results were obtained[10] for Au on W(110). One can, therefore, expect that the misfit between Au (or Ag) and W(110) may be relieved by the formation of a weakly incommensurate phase consisting of misfit dislocations along [001] separating larger areas which are nearly commensurate. This has been observed with STM for Au on W(110), where the complete monolayer grows almost pseudomorphic.[20] Note that the growth of Au on W(110) differs, however, from Ag on W(110). This is due to the fact that besides the fcc(111)/bcc(110) strain on the Au/W surface at increasing coverage gold introduces its own strain relaxation [which results in the well-known $22\times\sqrt{3}$ reconstruction at the (111) surface of bulk Au]. If most Ag atoms adsorb in commensurate sites, the photoemission data are subjected to a C_{2v} point-group symmetry. This is indeed observed and will be outlined in what follows.

Normal emission photoelectron spectra obtained for 1 ML Ag on W(110) with linearly polarized photons (energy $\hbar\omega$=21.2 eV) are reproduced in Fig. 5. Substrate emission occurs between E_F at initial state energy E_i=0 and about −3.3 eV. The strong peaks observed between −4 and −5 eV as well as broader features visible at −4.2 eV and −6.2 eV result from Ag. Based on an earlier interpretation[21] of Ag overlayers on Cu(100) and substantiated by our own polarization analysis we identify the peaks at −4.6 eV and −5.0 eV with emission from Ag *xz*, *yz* *d* orbitals. They are degenerate energetically under C_{6v} symmetry as expected for a free Ag(111) layer as well as C_{3v} point-group symmetry[22] for a Ag(111) surface. We emphasize, in particular, that photoemission intensities excited with *s*- or *p*-polarized light and observed in normal emission are independent of the light-incidence azimuth under C_{6v} or C_{3v} point-group symmetries. This is different in C_{2v} symmetry of the W(110) surface: orbitals with $xz(yz)$ symmetry can only be excited in normal emission by $x(y)$-polarized light. This selection rule is strictly valid only if spin-orbit coupling effects are neglected. This is not possible, since in Ag on W(110) the observed splitting of 0.4±0.1 eV is a nontrivial mixture of the net spin-orbit interaction (0.2 eV) and the effects of the crystal field. In the extreme case of purely relativistic point-group symmetries no polarization effects are predicted under C_{2v}. However, Fig. 5 clearly indicates an exchange of the intensities, when we switch from *s*-polarized light (field vector along *x*) to *p* polarization (y,z) with the light incidence plane along the $[1\bar{1}0]$ azimuth of W(110). This is a clear evidence that the emitting orbitals still retain some of their nonrelativistic orbital character. Most important in our context is that the role of *s* and *p* light are completely exchanged when the photons are incident in the [001] substrate azimuth. Then the spectrum excited with *s*-polarized light is almost identical to that observed with *p*-polarized light along $[1\bar{1}0]$. This observation is a unique fingerprint that the majority of Ag atoms are located in sites with approximate C_{2v} symmetry. According to the energy calculations mentioned already, the bcc site should then be populated preferentially.

Spectra taken at submonolayer Ag coverages between 0.13 ML and 1.0 ML are (except for intensities relative to substrate emission) identical within statistics with those shown in Fig. 5. Therefore, our analysis indicates that on W(110) at $\lesssim$1 ML the majority of Ag atoms adsorb at C_{2v} sites, most probably at the bcc site due to energy arguments. At this site Ag can shift slightly along $[1\bar{1}0]$ without energy costs to better adapt the misfit along $[1\bar{1}0]$. However, this works only for a finite number of sites and then the misfit must be released by a phase discommensuration along [001].

In their detailed LEED analysis Bauer and co-workers[7] observed that between 0.9 and 1.0 ML Ag the diffraction pattern changes continuously to that characteristic for the completed monolayer. For the 1 ML pattern the interpretation given in Ref. 7 assumes again a distorted and laterally rigid incommensurate lattice in an approximate Ag(111) geometry, but in contrast to the lattice at $<$1 ML now in the Kurdjumov-Sachs (KS) orientation. In this case the closed-packed rows Ag$[1\bar{1}0]$ of the monolayer are parallel to one of the close-packed substrate rows W$[\bar{1}11]$ or W$[1\bar{1}1]$. Note that this orientation is equivalent with Ag$[11\bar{2}]\|$W$[1\bar{1}2]$. As a consequence of this geometry a compression and concomitant strain release are expected along W$[1\bar{1}1]$ and equivalents, with troughs or ridges along W$[\bar{1}12]$, i.e., perpendicular to W$[1\bar{1}1]$. Our STM results for 1 ML are reproduced in Fig. 6. There is a clear corrugation pattern visible, with white lines in Fig. 6(a) oriented along W$[1\bar{1}2]$ and W$[\bar{1}12]$. Figure

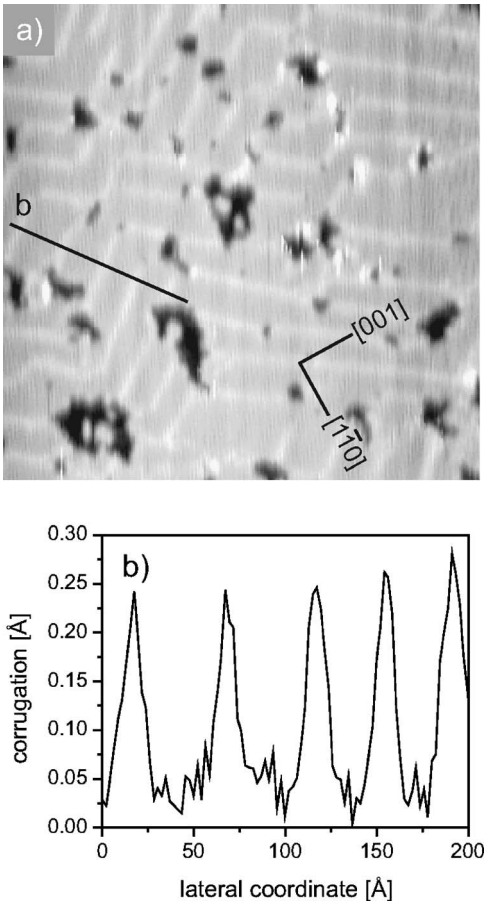

FIG. 6. At nearly 1 ML coverage STM shows an irregular soliton pattern imaged as white lines in (a). They are oriented preferentially along $[\bar{1}12]$ or $[1\bar{1}2]$ of W(110); the substrate coordinates are indicated. The corrugation measured along line b in (a) is reproduced in (b). Experimental parameters: −560 mV, 0.08 nA, and 520×520 Å^2.

6(b) shows the corrugation along the black line in Fig. 6(a). The layer is rather flat between these lines which appear with an average distance of about 43 Å. This fact and the scatter in the periodicity is an argument against a Moiré pattern as to be expected from a rigid adlayer lattice. In conclusion our results are consistent with the LEED pattern observed in, Ref. 7 but not with its interpretation.

Kim *et al.*[15] performed a very detailed STM study of the completed Ag monolayer on W(110). After Ag deposition at room temperature with growth rates (0.05–0.3 ML/min) smaller than in our experiments and annealing at ~330 K, they were able to obtain well ordered areas without any significant concentration of holes in the Ag film. Their samples clearly show very regularly spaced ridges along $[\bar{3}37]$ or $[3\bar{3}7]$, with a periodicity of about 31 Å perpendicular to $[\bar{3}37]$ and an experimental corrugation of 0.22 Å. As reported in Ref. 15 the size of domains with one orientation of the ridges is dependent on annealing. The W$[\bar{3}37]$ direction is rotated by 4° with respect to W$[\bar{1}12]$. Kim *et al.*[15] observe that in the Ag monolayer about 80% of the atoms are accomodated in pseudomorphic domains occupying bcc sites and the rest is forming misfit dislocations (or solitons in the language of the Frenkel-Kontorova model[23]) where the atoms are displaced from the W(110) bcc site. The preferential occupation of bcc sites is in perfect agreement with our polarization-dependent photoemission data combined with the binding energy calculations.[10]

The arrangement of the solitons is different in the two studies: While the gentle annealing performed in Ref. 15 led to a closed layer with stress relieve via a regular soliton pattern in $[\bar{3}37]$ or $[3\bar{3}7]$ directions, in the present nonannealed film partial stress release is obtained via persistent holes and in addition an irregular soliton pattern develops with the misfit dislocations preferentially oriented parallel to the $[\bar{1}12]$ and $[1\bar{1}2]$ directions. As evident from Fig. 6, the solitons are neither equidistant nor even parallel. These results can be qualitatively interpreted in the framework of the Frenkel-Kontorova model.[23] Within this model, the substrate is represented by a corrugation potential V and the adlayer by a harmonic interaction of strength K between the adatoms. For a small ratio V/K the adlayer remains rigid and incommensurate periodicities then give rise to a Moiré pattern. With increasing V/K it becomes energetically favorable to form commensurate domains separated by a soliton lattice which accommodates the misfit locally. In equilibrium, the soliton lattice is always periodic. However, if V/K is strong enough, equilibration of the misfit dislocations is kinetically hindered and a chaotic, disordered soliton lattice is formed.[24] In the present case the soliton mobility is small but nonnegligible at room temperature as reported in Ref. 15. Hence, small evaporation rate and gentle annealing allowed the formation of a regular soliton pattern in, Ref. 15 while in the present case the solitons are more or less trapped in a metastable, disordered configuration. Also, the misfit is not completely accommodated in the $[\bar{1}12]$ and $[1\bar{1}2]$ solitons, but is partially also released by the holes in the film. It is to be noted that the holes more or less replace the edge dislocations in the equilibrated Ag film, where the solitons switch between symmetry equivalent directions. For the closed Ag monolayer, equilibration obviously includes a slight rotation of the solitons by 4° from the $[\bar{1}12]$ and $[1\bar{1}2]$ directions into $[\bar{3}37]$ and $[3\bar{3}7]$, respectively. The periodicity of the solitons perpendicular to the $[\bar{3}37]$ and $[3\bar{3}7]$ directions is 31 Å, while the average spacing observed in our samples is 43 Å with a variation between 35 Å and 50 Å. The larger average spacing in the present study can be attributed to the partial stress release in the holes.

Kim *et al.*[15] report that annealing at 500 K transforms the ridge structure into a trough structure containing missing rows along the W[001] direction. The period is about 29 Å along the W$[\bar{1}10]$ direction. Most interesting here is their observation that the trough structure transforms slowly back to the ridge structure already at room temperature, directly demonstrating that there different structures occur with only a small difference in free energy. Transformation between these structures is slow around room temperature and therefore the film structure observed after deposition may be metastable, i.e., controlled by kinetics rather than free-energy minimization. The conclusion from this phase transformation

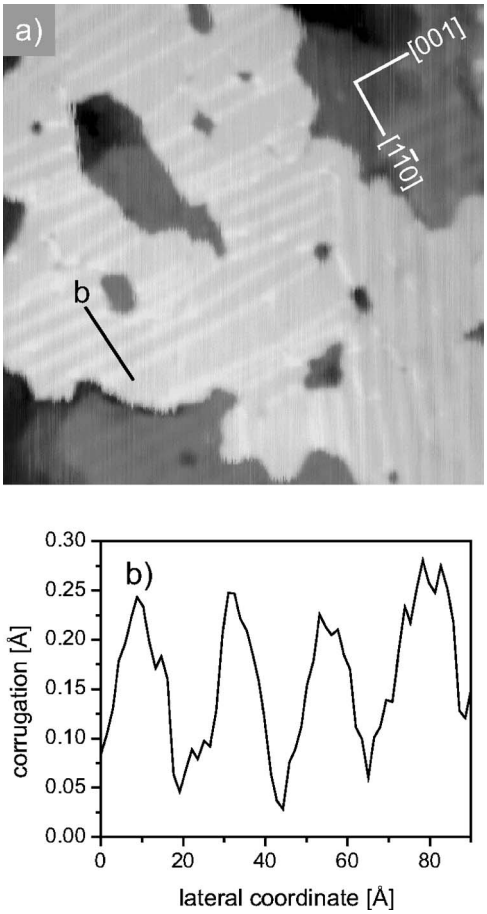

FIG. 7. STM results obtained at a nominal coverage of 1.5 ML Ag on W(110): 50% of the surface is covered by a bilayer [light in (a) and 50% by a monolayer (dark)]. Corrugation patterns are clearly resolved on the bilayer, measured corrugation along line b in (a) is shown in (b). Experimental parameters: 316 mV, 0.26 nA, 500×500 Å^2 in (a).

is unique: the ridge structure is more stable than the trough structure at room temperature. Kim *et al.*[15] estimate the energy barrier between the two structures to be (0.30 ± 0.07) eV, i.e., rather low. If we remember the energy calculation, which predicts the possibility to shift the Ag atoms in the bcc site by ±0.7 Å along $[1\bar{1}0]$ without significant energy cost, we can comprehend at least qualitatively why the structure observed in our data at coverages <1 ML converts into the ridge structure at 1 ML. We mention in this context that we never observed the ridge structure at submonolayer coverage.

If we increase the coverage above 1 ML, the subtle energy balance of the films is further modified. Figure 7 shows our STM results obtained at a nominal coverage of 1.5 ML. This means that 50% of W(110) is covered by a monolayer and 50% is covered by a bilayer. On the bilayer corrugation patterns are clearly resolved. In the left side of Fig. 7(a) we observe corrugation lines along W[001], with unequal spacing at an average periodicity of 24 Å, see Fig. 7(b). We did not observe any indications for transformation into the ridge pattern oriented along $[\bar{1}12]$ or $[\bar{3}37]$ as it occurs at 1.0 ML. The right part of Fig. 7(a) shows corrugation lines that run perpendicular to W$[1\bar{1}3]$, at a similar average distance as in the left part. With respect to the fcc lattice the solitons in both parts are parallel to the close packed rows, i.e. the fcc $[\bar{1}10]$ and $[10\bar{1}]$ directions. Thus one domain of the bilayer has again the Nishiyama-Wassermann orientation as observed for the submonolayer islands, while the other domains are symmetry equivalent with respect to the fcc lattice. This signals the transition from the W bcc substrate potential to the Ag fcc substrate potential. Obviously slight changes in the stress distribution tilt the balance back and forth between the two different orientations.

As mentioned in the Introduction, the Ag/W(110) system has also been investigated in a helium diffraction study by Engel and co-workers.[11] While these authors used the same Ag deposition rate of 0.7 ML/min as we used, their data show some agreement but also some differences if compared to Bauer *et al.*,[7] and the STM results obtained by Kim *et al.*[15] and our group. The buckling amplitudes observed in Ref. 11 are clearly less than expected from a hard-sphere model using a uniformly distorted Ag(111) plane for the Ag film. From this the authors conclude that local rearrangements must take place in the film. This is in agreement with the more recent studies. Also diffraction patterns are observed which, combined with a hard-sphere model, result in geometries not identical but similar to those obtained by Bauer *et al.* However, there are also some discrepancies. Engel's group reports a superstructure imposed to the substrate diffraction pattern between 0.2 and 1.5 ML, consisting of additional features in the $[1\bar{1}0]$ azimuth and optimally formed at just 1 ML. As the coverage is further increased, superstructure is seen rotated 32° off the $[1\bar{1}0]$ azimuth, with two equivalent domains, each exhibiting a 1D corrugation with an average periodicity of 22 Å. The first observation would be consistent with our results, if we assume an error in the coverage calibration of[11] which overestimates the coverage by about a factor of 2. However, such a big error is very improbable. The second diffraction pattern is not reproduced by any other experiment, even in case of a calibration error. We are left with the conjecture that due to different preparation conditions in the work of Engel *et al.*,[11] another structural phase of Ag on W(110) may have been produced.

IV. SUMMARY AND CONCLUSIONS

The present understanding of Ag growth on W(110) at room temperature can be summarized as follows. Already at low coverage, far below 1 ML, Ag atoms populate bcc sites of the substrate and form close-packed islands of monolayer thickness. Ag likes to form Ag(111)-like layers. However, due to a geometrical misfit with the W(110) surface stress is generated along W$[1\bar{1}0]$. This is released by the formation of solitons, which run parallel to W[001] and are observed with a distance between about 25 Å and 30 Å, depending on the very details of the growth process. The rotation of the submonolayer islands conforms to the Nishiyama-Wassermann orientation.

With increasing coverage the packing density increases, and at 1 ML, while the majority of Ag atoms still reside in

bcc substrate positions, the strain release pattern changes: the ridges now are aligned along $[\bar{3}37]$ or $[\bar{1}12]$ at an average distance of about 35,...,50 Å conforming to a Kurdjumov-Sachs orientation. The details of the soliton arrangement depend on the degree of equilibration and the presence or absence of holes in the film which allow an additional stress release. Within the ridges Ag atoms populate incommensurate sites such as bridge and quasi-three-fold hollow positions. Between the ridges, the majority of atoms populate the bcc sites of W(110) and form an almost commensurate overlayer. Annealing a complete monolayer changes the stress relieve pattern again, as reported in detail in Ref. 15. After completion of the first ML, a second monolayer starts to grow by formation of islands which increase in diameter with coverage. As the Ag coverage is increased from 1 to 1.5 ML, i.e., as extended areas with bilayer coverage are formed, the strain relieve pattern returns to the Nishiyama-Wassermann orientation. The corrugation lines or solitons are oriented along W[001] as in the submonolayer, but other orientations appear as well, which are not symmetrically equivalent with respect to the W bcc directions, but symmetrically equivalent to the Ag fcc directions, thus indicating the transition from the W substrate potential to the Ag potential seen by the second Ag layer. Obviously the different strain release patterns differ not significantly in energy. This explains their rapid change with coverage. An interesting property of the Ag/W(110) system is the (slow) mobility of the solitons at room temperature which allows us to study both ordered and disordered soliton lattices as well as the phase transitions between the different arrangements. The various and partially conflicting structures reported in the literature thus turn out to be due to a multitude of energetically almost degenerate arrangements that are determined by kinetic parameters (temperature and deposition flux) on the one hand, and a subtle competition between normal and lateral interactions changing within the coverage range between 0.1 and 2 ML of Ag on the other hand. While the majority of Ag atoms resides in bcc sites in all the observed structures, the energetic differences stem essentially from different soliton patterns.

ACKNOWLEDGMENTS

The experiments performed in Kassel were supported continuously by the Deutsche Forschungsgemeinschaft (DFG); those in Innsbruck by the Austrian Science Fund (FWF). We thank K. Berge, A. Gerlach, and W. Holzapfel for their help in taking data.

[1] J. H. van der Merwe, E. Bauer, D. L. Tönsing, and P. M. Stoop, Phys. Rev. B **49**, 2127 (1994).
[2] I. V. Markov, *Crystal Growth for Beginners* (World Scientific, Singapore, 1995), Chap. 4.
[3] H. Brune, Surf. Sci. Rep. **31**, 121 (1998).
[4] N. Memmel, Surf. Sci. Rep. **32**, 91 (1998).
[5] M. Gsell, P. Jakob, and D. Menzel, Science **280**, 717 (1998).
[6] J. A. Rodriguez, Surf. Sci. Rep. **24**, 223 (1996).
[7] E. Bauer, H. Poppa, G. Todd, and P. R. Davis, J. Appl. Phys. **48**, 3773 (1977).
[8] E. Bauer, Appl. Surf. Sci. **11**, 479 (1982).
[9] E. Bauer and H. Poppa, Thin Solid Films **121**, 159 (1984).
[10] H. Gollisch, Surf. Sci. **175**, 249 (1985).
[11] Y. Yang, H. Xu, and T. Engel, Surf. Sci. **276**, 341 (1992).
[12] A. Elbe, G. Meister, and A. Goldmann, Surf. Sci. **397**, 346 (1998).
[13] J. Feydt, A. Elbe, H. Engelhard, G. Meister, and A. Goldmann, Surf. Sci. **452**, 33 (2000).
[14] M. Bürgener, W. Holzapfel, G. Meister, and A. Goldmann, Surf. Sci. **495**, 129 (2001).
[15] T.-H. Kim, B.-Y. Choi, Y. J. Song, W. G. Park, S.-J. Kahng, and Y. Kuk, Phys. Rev. B **67**, 233401 (2003).
[16] M. Bode, R. Pascal, and R. Wiesendanger, Surf. Sci. **344**, 185 (1995).
[17] R. Matzdorf, A. Gerlach, R. Hennig, G. Lauff, and A. Goldmann, J. Electron Spectrosc. Relat. Phenom. **94**, 279 (1998).
[18] A. Elbe, Dissertation, University of Kassel, 1997.
[19] E. Bauer and J. H. van der Merwe, Phys. Rev. B **33**, 3657 (1986).
[20] M. L. Hildner, K. E. Johnson, and R. J. Wilson, Surf. Sci. **388**, 110 (1997).
[21] J. G. Tobin, S. W. Robey, and D. A. Shirley, Phys. Rev. B **33**, 2270 (1986).
[22] W. Eberhardt and F. J. Himpsel, Phys. Rev. B **21**, 5572 (1980).
[23] P. Bak, Rep. Prog. Phys. **45**, 587 (1982).
[24] C. Deisl, K. Swamy, R. Beer, A. Menzel, and E. Bertel, J. Phys.: Condens. Matter **14**, 4199 (2002).
[25] R. Q. Hwang, J. Schröder, C. Günther, and R. J. Behm, Phys. Rev. Lett. **67**, 3279 (1991).
[26] K. Thürmer, E. D. Williams, and J. E. Reutt-Robey, Phys. Rev. B **68**, 155423 (2003).
[27] K. Wandelt, in: *Thin Metal Films and Gas Chemisorption*, edited by P. Wissmann (Elsevier, Amsterdam, 1987), pp. 280–368.